Title

Local entanglement and confinement transitions in the random transverse-field Ising model on the pyrochlore lattice

Permalink

Journal

ISSN

Authors

Pardini, Tom
Menon, Anirudha
Hau-Riege, Stefan P
et al.

Publication Date

DOI

Peer reviewed

Local entanglement and confinement transitions in random transverse-field Ising model on the pyrochlore lattice

Tom Pardini,[1] Anirudha Menon,[2] Stefan P. Hau-Riege,[1] and Rajiv R. P. Singh[2]

[1]*Lawrence Livermore National Laboratory, 7000 East Ave. Livermore, CA 94550*
[2]*Department of Physics, University of California Davis, CA 95616, USA*

(Dated: October 15, 2019)

We use Numerical Linked Cluster Expansions (NLC) and Exact Diagonalization (ED) to study confinement transitions out of the Quantum Spin Liquid (QSL) phase in the pyrochlore-lattice Ising antiferromagnet with random transverse fields. We calculate entanglement entropies associated with local regions defined by single tetrahedra to observe these transitions. The randomness-induced confinement transition is marked by a sharp reduction in the local entanglement and a concomitant increase in Ising correlations. In NLC, it is studied through the destruction of loop resonances due to random transverse-fields. The confining phase is characterized by a distribution of local entanglement entropies, which persists to large random fields.

PACS numbers: 74.70.-b,75.10.Jm,75.40.Gb,75.30.Ds

In recent years, many candidate quantum spin-liquid (QSL) materials have been identified [1–7]. A characteristic of QSLs is the high degree of quantum entanglement, allowing them to host fractionalized quasiparticles. However, a convincing experimental demonstration of QSL remains elusive. Part of the difficulty lies in the nature of the phase, which does not have a measurable order parameter. Emergent, fractionalized degrees of freedom do not directly couple to external probes. Thus, with few exceptions, such as quantized thermal hall effect [8], most experimental signatures of QSL are indirect and subject to alternative interpretations. Impurities, which are ever present in condensed matter systems, play a significant role in shaping the macroscopic phases and understanding them is important for establishing a QSL experimentally [9–16].

One class of materials that have attracted significant interest are the spin-ice family of rare-earth pyrochlores [17–25]. Magnetic rare-earth ions form a lattice of corner-sharing tetrahedra. Though these ions typically have large spin, strong spin-orbit coupling and crystal-field effects map them on to an effective two-state or spin-half system. The local Ising axis is defined by the line joining the vertex to the center of the tetrahedron. When exchange interactions favor '2-in-2-out' Ising states in each tetrahedron, this leads to macroscopic ground state degeneracy classically with the well-known Pauling entropy [26]. This classical spin-liquid, also called spin-ice, is well established in some rare earth pyrochlores [18].

These materials can be divided into Kramers and non-Kramers systems [17]. The former consist of odd number of electrons per ion which must have a two-fold degeneracy for every single-ion eigenstate. The latter will typically have non-degenerate eigenstates and double degeneracy can only arise as a result of some lattice symmetry. Thus spin-active non-Kramers systems can arise from two nearby non-degenerate states well separated from the rest, or, from a lattice-symmetry protected dou-
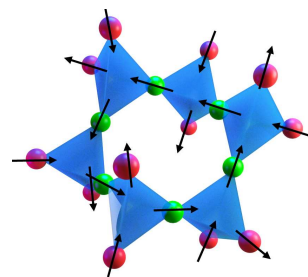

FIG. 1: Cluster of 6 tetrahedra connected in a ring. The six interior sites of the cluster are denoted by green circles and the 12 boundary sites are denoted by red circles. The arrows denote one spin-ice configuration for the cluster.

blet ground state which will be split by impurities. These systems can be modelled by random-transverse field Ising models [27–32]. Indeed the material $Pr_2Zr_2O_7$ is a realization of this model [33].

Here we study the quantum Ising-antiferromagnet on the pyrochlore lattice by Numerical Linked Cluster (NLC) expansions [34–36] and exact diagonalization (ED). We focus on the local entanglement properties of the system and examine their behavior at the confinement transitions. We find that entanglement of spins of a tetrahedron with the rest of the system contains sharp changes associated with different confining transitions.

A simple NLC calculation diverges inside the QSL phase. To obtain convergent results, one must consider each cluster as embedded in a superposition of spin-ice states. The confinement transition can be observed by studying the destruction of ring-exchange resonance due to the random fields. A modification of Benton's perturbative argument [28] shows that at the phase boundary the width of the transverse-field distribution scales quadratically with the mean value in agreement with the NLC results. We also find that the confining phase [32]
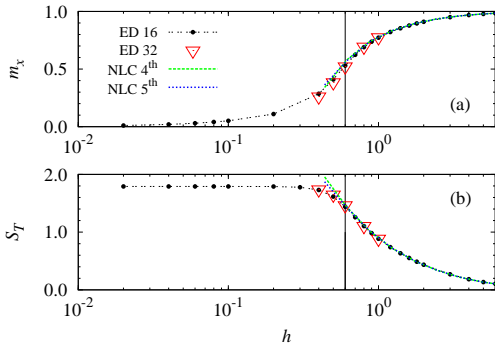
FIG. 2: (a) Expectation value of spin along the transverse field m_x, and (b) Single-tetrahedron entanglement entropy S_T, as a function of the transverse-field h with no disorder. The data is for 16 and 32-site clusters and 4th and 5th order NLC. The vertical black lines denote the transition point [30, 31] between QSL and the paramagnetic phase. NLC does not converge within the QSL phase, and for this reason NLC results are not shown for small h values.
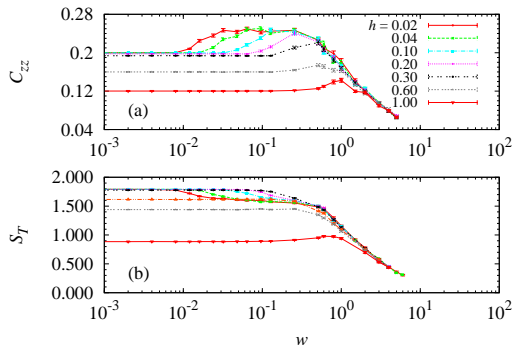

FIG. 3: (a) Ising correlations C_{zz}, and (b) Single-tetrahedron entanglement entropy S_T as a function of width of the field distribution w for different mean values of the field h. Data have been obtained via ED on a 16-site cluster, and each data point represents an average over 100 independent disorder configurations. Error-bars are from finite sampling of disorder.

is characterized by a broad distribution of local entanglement entropies, a property which persists to high random fields. This means that even with increasing random fields there will be pockets of strong entanglement with local behavior of a QSL.

We consider the Hamiltonian

$$\mathcal{H} = J \sum_{<i,j>} \sigma_i^z \sigma_j^z - \sum_i h_i \sigma_i^x, \qquad (1)$$

where $J = 1$, and the transverse fields h_i are independent Gaussian random variables with mean h and standard deviation w. On a finite cluster with periodic boundary conditions, we calculate the ground state wavefunction of

the system. We divide the system into two parts A and its complement B. Let the reduced density matrix of A be ρ_A. The von-Neumann entanglement entropy between A and its complement B is:

$$S_A = S_B = - \operatorname{Tr} \rho_A \ln \rho_A. \qquad (2)$$

In this work, A is made up of the four spins belonging to any single tetrahedron, and B is made up of all the remaining spins. This leads to the definition of single-tetrahedron entanglement entropy

$$S_T = [- \operatorname{Tr} \rho_T \ln \rho_T]. \qquad (3)$$

The square brackets indicate that the quantity is averaged over the tetrahedra in the cluster and over disorder configurations. In addition, we study the average moment along the local field, defined as

$$m_x = [\frac{1}{N} \sum_i |\langle \sigma_i^x \rangle|]. \qquad (4)$$

Here N is number of sites and the angular brackets throughout this study refer to ground state expectation values, while the square brackets refer to an average over disorder configurations. We also calculate the correlation sum for the Ising components:

$$C_{zz} = [\frac{1}{N(N-1)} \sum_{i,j \neq i} |\langle \sigma_i^z \sigma_j^z \rangle|], \qquad (5)$$

where the sum is over all pairs of spins.

To obtain the results in the thermodynamic limit, we turn to NLC [34–36]. An extensive property of interest P, per site, can be calculated by a sum over connected clusters c that can be embedded in the lattice.

$$P/N = \sum_c L(c) \times W(c), \qquad (6)$$

where $L(c)$ is the lattice constant of the cluster, or the number of times the cluster arises in the lattice per site. The weight $W(c)$ is defined recursively as

$$W(c) = P(c) - \sum_s W(s), \qquad (7)$$

where $P(c)$ is the property for the cluster and the subtraction is over subclusters.

To study property of spin-ice systems, it is useful to consider clusters made up of full tetrahedra [37, 38]. To 5th order, that is up to 5 tetrahedra, there are a total of 8 clusters. We include a 9th cluster, consisting of six tetrahedra in a ring, shown in Fig. 1, as it plays a special role in the spin-ice phase.

We begin with results for the uniform system ($w = 0$). In Fig. 2, the expectation value of the spin along the transverse field and the local entanglement entropy associated with a single tetrahedron are shown as a function of the field. The 4th and 5th order NLC results are

indistinguishable in the plot in the high-field paramagnetic phase, showing that they represent the results in the thermodynamic limit. The ED results for 16− and 32−site clusters are also shown. In the thermodynamic limit, there may be a small discontinuity at the transition [30, 31], but finite size effects are small in the paramagnetic phase right down to the transition. This first order transition point from previous studies [30, 31] is indicated by the vertical black lines.

While the simple NLC converges well in the high-field phase right up to the transition, it diverges in the QSL phase and we need to modify it for the QSL. The physics of QSL is lost by having fluctuating spins at the boundary of the finite clusters. This is because every spin must be part of two tetrahedra in order to not mix different ice states by local fluctuations. But the boundary spins of a cluster belong to only one. Thus, two boundary spins in the same tetrahedron can be flipped to go from one ice configuration to another already in order h^2. This is clearly incorrect.

In order to fix this problem we adopt a modified NLC scheme. We envisage local fluctuations in the interior of the QSL. Each cluster is divided into interior and boundary spins depending on whether or not the spin belongs to two or one tetrahedron in the finite cluster (See Fig. 1). The boundary spins feel additional longitudinal fields, coming from tetrahedra external to the cluster. It can be shown that the modified NLC in 5th order gives perturbative properties correct to order h^8 except for the ring exchanges. However, these perturbative terms generate very small entanglement at small fields and ring exchanges are key to the physics of the QSL [21–23].

In order to capture the physics of ring exchanges one must consider clusters where tetrahedra form rings. All the order one entanglement for small h arises from ring exchanges [23, 30]. This resonance can be destroyed by random fields, effectively killing the superposition and consequential entanglement. For studying this, cluster 9 consisting of six tetrahedra in a ring shown in Fig. 1 plays a crucial role.

In this cluster, each tetrahedron has two interior and two boundary spins. In our modified NLC, the cluster is embedded in a larger system. The Ising couplings of the spins external to the cluster result in longitudinal fields on the boundary spins of the cluster. The problem divides into different sectors corresponding to different boundary longitudinal fields. The key sector is one where in each tetrahedron one boundary spin has a positive and the other negative longitudinal field. At low energies this sector maps on to an effective 2−level system given by the two alternating spin configurations along the hexagon of the cluster.

For a uniform system, this leads to an entanglement entropy for each tetrahedron of $\ln 2$ in the sector where the resonance occurs, and zero in all other sectors apart from small perturbative corrections. Thus a sum over all tetra-
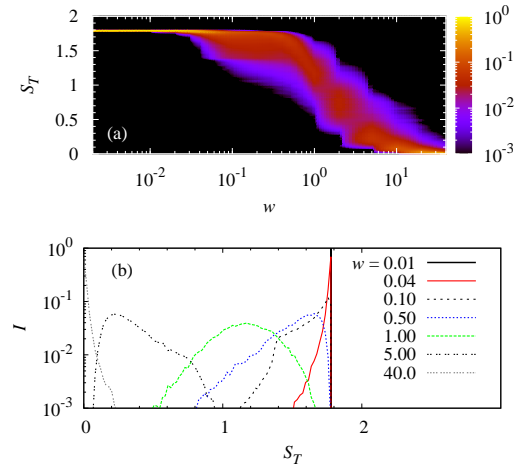

FIG. 4: (a) Distribution of single-tetrahedron entanglement entropy S_T for $h = 0.1$ and various w values. The color scale represents the normalized intensity I. (b) Several cuts of the intensity I in (a) for selected w values. For $w = 0.01$, the intensity is a delta function shown as a solid black line at $S_T \sim 1.77$.

hedron gives $6 \ln 2$ in the resonating sector. The cluster has 730 total spin-ice states, 128 of which lead to the resonating state. If we assume that each one of the spin-ice states must be weighted with equal probability in the interior of the spin-ice as expected at the Rokhsar-Kivelson (RK) point [39], the weight of this cluster for the entanglement entropy per tetrahedron becomes $(6 \times 128/730) \ln 2$. This cluster has a count of one per site or two per tetrahedron. Thus, multiplying the weight by a factor of 2 gives an entanglement entropy for a tetrahedron in the thermodynamic system to be approximately 1.5. Our ED estimate for the low field entanglement entropy shown in Fig. 2 is less than 20 percent higher than this. The comparison suggests that the resonating configurations are enriched relative to others by less than 20 percent with respect to the RK point in the model. This is consistent with the Monte Carlo study of the ring-exchange model [23].

We now turn to the main focus of our study with random transverse fields. The Ising correlation sum and tetrahedron entanglement entropy from ED are shown in Fig. 3, where we see that an increase in the Ising correlation occurs concomitant with a decrease in local entanglement entropy. This shows that the confinement transition is associated with the lifting of degeneracy in the spin-ice subspace and leads to the development of Ising correlations [32]. Fig. 4 shows the distribution of single-tetrahedron entanglement entropies. One finds that as soon as one enters the confining phase the entanglement entropy develops a broad distribution. Fig. 4b shows a few cuts through the distribution function. In

the QSL phase the entanglement entropy is essentially a delta function. In the confining phase it is broad. for the finite system, there remains weight at the largest value until one gets into a paramagnetic phase around $w = 0.5$ after which the peak gradually moves to smaller values. However, the distribution remains broad all the way up to large randomness.

Note that ED cannot give the correct thermodynamic phase boundary because our cluster has loops of length 4 coming from periodic boundary conditions. These small loops lead to a phase boundary where w scales linearly with h.

To study the phase boundary for the thermodynamic system, we must use NLC and focus on cluster 9. The tetrahedron entanglement entropy in the resonating sector of cluster 9 is shown in Fig. 5. We see that the resonance, which leads to an entanglement of $\ln 2$ is killed with disorder. To further understand this, we turn to perturbation theory [28]. With disorder, the two-state problem for the cluster can be described by an effective Hamiltonian

$$H_{\text{eff}} = a\sigma_x + b\sigma_z, \qquad (8)$$

where $a = \frac{63}{256}h^6$, while

$$b = \frac{1}{48}\sum_t (h_{i1}^2 - h_{i2}^2)(h_{b1}^2 - h_{b2}^2), \qquad (9)$$

where the sum is over all six tetrahedra. Here, h_{i1} and h_{i2} are the random-fields at the interior sites and h_{b1} and h_{b2} the random fields at the two boundary sites of the tetrahedra. Benton had argued [28] that the average degeneracy lifting perturbation should scale as wh^3. However, as seen from Eq. 8, there are two cancellations in each tetrahedron and b must vanish as w^2. We find that for Gaussian disorder it scales approximately as $14.7w^2h^2$. Calling the point $a = b$ as the transition point gives the phase boundary $w = ch^2$, with $c \approx 0.90$. This phase boundary is also shown in the inset of Fig. 5 and agrees well with our calculations, where the transition is determined by the horizontal dashed line corresponding to an S_T of 0.4165 as appropriate for $a = b$ in Eq. 7.

A sketch of the phase diagram is shown in Fig. 6 with QSL, Paramagnetic (PM), Ising (I) and Griffiths-McCoy (GM) phases. The Ising phase is characterized by enhanced random Ising correlations, whereas the Griffiths-McCoy phase is characterized by only pockets of entanglement corresponding to rare regions in the disorder configuration. The PM-QSL boundary is indicated to be vertical. NLC results differ sharply from ED, even with non-zero w, around $h = 0.6$. Whether the phase immediately to the left of the boundary is a true thermodynamic QSL or an inhomogeneous Griffiths-McCoy like phase [40] with only pockets of high entanglement deserves further attention. The paramagnetic phase boundary at large w is roughly horizontal. Various properties
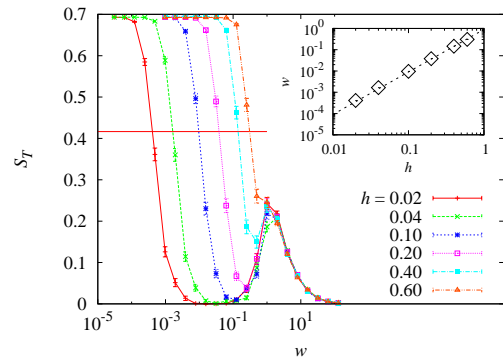

FIG. 5: Single-tetrahedron entanglement entropy S_T obtained from cluster 9 as a function of width w for different h values. Each data point represents an average over 200 independent disorder configurations. The horizontal line corresponds to $S_T = 0.4165$. The inset shows the transition point obtained from these calculations (diamonds) and from perturbation theory (dashed line).
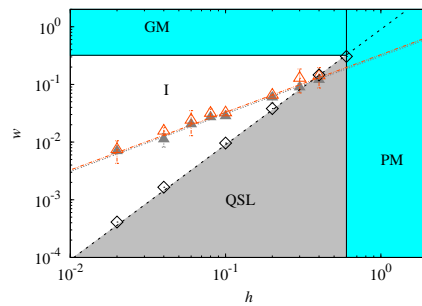

FIG. 6: A sketch of the phase diagram for the random transverse-field Ising model with QSL, paramagnetic (PM), Ising (I), and Griffiths-McCoy (GM) phases. The triangles represent confinement phase boundary on the finite cluster. The diamonds are obtained from NLC and represent the phase boundary in the thermodynamic limit.

collapse on a single scaling curve at larger w implying a predominantly local paramagnetic behavior. The confinement transition due to randomness, obtained in the finite cluster study from Ising correlations and entanglement entropy respectively are shown by open and closed triangles. The thermodynamic phase boundary, where hexagonal loop resonances are lost, is shown by diamonds and perturbation theory results are indicated by a dashed line. The nature of the phase transition and the possibility of a long-ranged spin-glass phase deserves further consideration [41].

To summarize, we have studied the random transverse-field Ising model on the pyrochlore lattice using NLC and ED. This model has a deconfined QSL phase, which is subject to two types of confining transitions [32]. Large transverse-fields lead to confinement where spins

are locked along the field direction. On the other hand, a distribution of random fields leads to a selection within the ice manifold also leading to a loss of entanglement and confinement. We have shown that local entanglement associated with spins in a tetrahedron contains sharp changes associated with these transitions.

Simple NLC converges well in the high-field phase, right up to the transition. But, it diverges in the QSL. The QSL phase can be studied within NLC by embedding each cluster inside a spin-ice. Nearly all the entanglement in the QSL phase arises from ring-exchange resonances. These can be frozen by random transverse-fields leading to confinement.

In the confining phase, there is a distribution of local entanglement entropies, a property which persists to large random fields. Experiments on $Pr_2Zr_2O_7$ found rather large randomness [33], implying that the system can at best have pockets of high entanglement. Improvement in material preparation should lead to reduced disorder. Our work provides quantitative estimates of how much randomness needs to be lowered to obtain a true QSL phase.

It would be interesting to extend these studies to random XXZ and other models of quantum spin-ice, where many other varieties of quantum spin-liquid phases are known to exist [42].

---

[1] L. Balents, Nature **464**, 199 (2010).

[2] L. Savary, and L. Balents, Rep. Prog. Phys. 80, 016502 (2017).

[3] T. H. Han, J. S. Helton, S. Y. Chu, D. G. Nocera, J. A. Rodriguez-Rivera, C. Broholm and Y. S. Lee, Nature 492, 406 (2012); M. Fu, T. Imai, T.-H. Han, Y. S. Lee, Science 350, 655-658 (2015).

[4] Y. Shen, Y.-D. Li, H. Wo, Y. Li, S. Shen, B. Pan, Q. Wang, H. C. Walker, P. Steffens, M. Boehm, Y. Hao, D. L. Quintero-Castro, L. W. Harriger, M. D. Frontzek, L. Hao, S. Meng, Q. Zhang, G. Chen, J. Zhao, Nature 540, 559-562 (2016); Y. D. Li, Y.-M. Lu, G. Chen, Phys. Rev. B 96, 054445 (2017); Z. Zhu, P. A. Maksimov, S. R. White, A. L. Chernyshev, Phys. Rev. Lett. 120, 207203 (2018).

[5] G. Jackeli, and G. Khaliullin, Phys. Rev. Lett. 102, 017205 (2009).

[6] J. G. Rau, E. K.-H. Lee, and H.-Y. Kee, Phys. Rev. Lett. 112, 077204 (2014). S. M. Winter, K. Riedl, D. Kaib, R. Coldea, and R. Valenti, Phys. Rev. Lett. 120, 077203 (2018).

[7] A. Banerjee, C.A. Bridges, J-Q. Yan, A.A. Aczel, L. Li, M.B. Stone, G.E. Granroth, M.D. Lumsden, Y. Yiu, J. Knolle, D.L. Kovrizhin, S. Bhattacharjee, R. Moessner, D.A. Tennant, D.G. Mandrus, S.E. Nagler, Nature Materials 2016, 15, 733–740.

[8] Y. Kasahara, T. Ohnishi, Y. Mizukami, O. Tanaka, Sixiao Ma, K. Sugii, N. Kurita, H. Tanaka, J. Nasu, Y. Motome, T. Shibauchi, Y. Matsuda, Nature 559, 227-231 (2018).

[9] I. Kimchi, A. Nahum and T. Senthil, Phys. Rev. X 8, 031028 (2018).

[10] Z. Zhu, P. A. Maksimov, S. R. White, A. L. Chernyshev, Phys. Rev. Lett. 119, 157201 (2017).

[11] J. Knolle, R. Moessner, N. B. Perkins, cond-mat arXiv:1807.09670.

[12] K. Uematsu, and H. Kawamura, cond-mat/arXiv:1807.08417.

[13] K. Uematsu, H. Kawamura, J. Phys. Soc. Jpn. 86. 044704 (2017).

[14] E. C. Andrade, J. A. Hoyos, S. Rachel, and M. Vojta, Phys. Rev. Lett. 120, 097204 (2018).

[15] R. R. P. Singh, Phys. Rev. Lett. 104, 177203 (2010).

[16] I. Rousochatzakis, S. R. Manmana, A. M. Lauchli, B. Normand, and F. Mila, Phys. Rev. B 79, 214415 (2009).

[17] M. J. P. Gingras, in *Introduction to Frustrated Magnetism*, (Springer, 2011) arXiv:0903.2772 .

[18] A. P. Ramirez, A. Hayashi, R. J. Cava, R. Siddhartan and B. S. Shastry, Nature 399, 333-335 (1999).

[19] K. A. Ross, L. Savary, B. D. Gaulin and L. Balents, Phys. Rev. X 1, 021002 (2011).

[20] L. Savary and L. Balents, Phys. Rev. Lett. 108, 037202 (2012).

[21] M. Hermele, M.P.A. Fisher, and L. Balents, Phys. Rev. B 69, 064404 (2004).

[22] A.H. Castro Neto, P. Pujol, and E. Fradkin, Phys. Rev. B **74**, 024302 (2006).

[23] N. Shannon, O. Sikora, F. Pollmann, K. Penc, and P. Fulde, Phys. Rev. Lett. **108**, 067204 (2012).

[24] A. Banerjee, S. V. Isakov, K. Damle and Y. B. Kim, Phys. Rev. Lett. **100**, 047208 (2008);

[25] M. Taillefumier, O. Benton, H. Yan, L. D. C. Jaubert, N. Shannon, Phys. Rev. X 7, 041057 (2017).

[26] L. Pauling, J. Am. Chem. Soc. **57**, 2680 (1935).

[27] L. Savary, and L. Balents, Phys. Rev. Lett. 118, 087203 (2017).

[28] O. Benton, Phys. Rev. Lett. 121, 037203 (2018).

[29] R. Moessner, S. L. Sondhi, and E. Fradkin, Phys. Rev. B 65, 024504 (16 pages) (2002).

[30] J. Rochner, L. Balents and K. P. Schmidt, Phys. Rev. B 94, 201111 (2016).

[31] P. Emonts and S. Wessel, Phys. Rev. B 98, 174433 (2018).

[32] G. Chen, Phys. Rev. B 94, 205107 (2016).

[33] J.-J. Wen, S. M. Koohpayeh, K. A. Ross, B. A. Trump, T. M. McQueen, K. Kimura, S. Nakatsuji, Y. Qiu, D. M. Pajerowski, J. R. D. Copley, C. L. Broholm Phys. Rev. Lett. 118, 107206 (2017).

[34] M. Rigol, T. Bryant, R. R. P. Singh, Phys. Rev. Lett. 97, 187202 (2006); ibid. Phys. Rev. E 75, 061118 (2007).

[35] A. B. Kallin, K. Hyatt, R. R. P. Singh, R. G. Melko, Phys. Rev. Lett. 110, 135702 (2013).

[36] B. Tang, E. Khatami, M. Rigol, Computer Physics Communications 184, 557-564 (2013).

[37] R. Applegate, N. R. Hayre, R. R. P. Singh, T. Lin, A. G. R. Day, M. J. P. Gingras, Phys. Rev. Lett. 109, 097205

(2012); N. R. Hayre, K. A. Ross, R. Applegate, T. Lin, R. R. P. Singh B. D. Gaulin, M. J. P. Gingras, Phys. Rev. B 87, 184423 (2013).

[38] H. Changlani, cond-mat/arXiv:1710.02234.

[39] D. Rokhsar and S. Kivelson, Phys. Rev. Lett. 61, 2376 (1988).

[40] R. B. Griffiths, Phys. Rev. Lett. 23, 17 (1969); B. M. McCoy, Phys. Rev. 188, 1014 (1969).

[41] A. Andreanov, J. T. Chalker, T. E. Saunders, D. Sherrington, Phys. Rev. B 81, 014406 (2010).

[42] O. Benton, L. D. C. Jaubert, R. R. P. Singh, J. Oitmaa, N. Shannon, Phys. Rev. Lett. 121, 067201 (2018).